TITLE:

Discovery of a novel mesothelin specific human antibody VH domain

Zehua Sun[1]#*, Xiaojie Chu[1]#, Cynthia Adams[2]#, Tatiana V. Ilina[3], Sandra Vergara[3], Chuan Chen[1], Dontcho Jelev[1], Rieko Ishima[3], Wei Li[1], John W Mellors[12], Guillermo Calero[3]*, Dimiter S Dimitrov[12]*

1 Center for Antibody Therapeutics, Division of Infectious Diseases, Department of Medicine, University of Pittsburgh Medical School, 3550 Terrace St., Pittsburgh, PA 15261, USA

2 Abound Bio, 1401 Forbes Ave., Pittsburgh, PA 15219, USA

3 Department of Structural Biology, University of Pittsburgh School of Medicine, Pittsburgh, PA, USA.

*corresponding author.

Authors contribute equally to the manuscript.

ABSTRACT

Antibody based therapeutics targeting mesothelin (MSLN) have shown limited anti-tumor activities in clinical trials. Novel antibodies with high affinity and better therapeutic developability properties are needed as preclinical candidates. In the present study, we have isolated and characterized a novel VH domain 3C9 from a large size human immunoglobulin heavy chain variable (VH) domain library. 3C9 exhibited high affinity [KD (dissociation constant) < 3nM] and demonstrated good specificity in a membrane proteome array (MPA). Both CAR-T cells and antibody domain drug conjugations (DDCs) generated with 3C9, showed effective killing of MSLN positive cells *in vitro* without off-target effects. This is also the first report of the crystal structure of MSLN based on the analysis of the MSLN-3C9 complex which was solved at 2.9 Å resolution. The newly identified antibody domain is a promising candidate therapeutic against cancer.

Running title: MSLN specific antibody VH domain

Key words: antibody VH domain, MSLN, structure, CAR-T and ADCs.

Introduction

Mesothelin (MSLN) is a validated and attractive tumor-associated antigen identified for antibody based therapy against multiple solid tumors with MSLN expression [1-9]. Several antibody therapeutics including Immunotoxins, chimeric antigen receptor t-cells (CAR-Ts) and antibody drug conjugates (ADCs) have been evaluated and show limited anti-tumor activities in clinical trials [10-12], indicating an urgent need for novel therapy designs and isolation of MSLN specific antibodies. There are several principal challenges in the development of antibody therapeutics against MSLN expressing solid tumors: (1) the antibody affinity/avidity which can allow recognition of tumor cells with low surface density of MSLN; (2) the antigen specificity to direct antibody therapeutics to target cells without off-target killing effects; (3) the antibody penetration of solid tumors and (4) the aggregation profile of the antibody.

Since the first antibody domain Caplacizumab was approved by the FDA in 2019, VH antibody domains have been widely discussed for their multiple advantages over traditional antibodies, especially their reduced immunogenicity (fewer epitopes), and better penetration of solid tumors [13, 14]. Antibody domains, which are about 10 times smaller than full length IgGs, could have up to a 100-fold higher effective diffusion coefficient in tumors [15]. However, their half-life in circulation is much shorter than that of full-size antibodies and they can be cleared quickly if binding to the target is not of very high affinity. Based on these limitations, isolation and characterization of novel antibody domains with high affinity and engineering potential will be beneficial for the development of therapies against MSLN. To date, there is no domain antibody reported that is qualified for clinical trials against MSLN positive solid tumors.

Previously, we constructed a large scale human antibody VH domain library based on thermo-stable anti-aggregation scaffolds for phage display [16, 17]. Panels of binders were isolated from this antibody VH domain library against different targets, demonstrating the quality and diversity of the library. In the present study, we discuss the isolation and characterization of a novel MSLN specific antibody domain 3C9 with high affinities (KD < 3 nM). 3C9 demonstrates satisfactory properties of specificity with no off-target activity detected in a MPA assay screening around 6,000 different membrane associated surface proteins. 3C9 based ADC and CAR-T cells are effective in mediating cytotoxicity in MSLN positive tumor cells without off-target effects, and can be potentially used for pre-clinical trials against different models of mesothelin expressing cancers. We also characterize the unique binding site of 3C9 to MSLN, which is different than the Phase II trial candidate, Amatuximab. This is the first report of the full length MSLN structure, achieved by crystallization of the MSLN-3C9 complex.

Results:

Identification and characterization of a novel human MSLN-specific VH antibody domain.

We constructed human recombinant MSLN proteins, which were used as antigens to isolate MSLN-specific binders from a large size human antibody VH domain library by phage display. This strategy yielded a panel of unique domains with the affinities ranging from 0.5 nM to 200 nM for human MSLN. We extensively characterized one VH domain, nominated 3C9, which showed very good aggregation resistance ([18], and figure 1A). In an ELISA assay, 3C9 exhibited an EC_{50} less than 10 nM (Figure 1B). In a Surface Plasmon Resonance (SPR) assay, 3C9 exhibited a high affinity to human MSLN with the equilibrium dissociation constant (KD) less than 3 nM (Figure 1D). VH 3C9 also binds macaque MSLN, though with a lower binding affinity (data not shown).

To measure the effect of avidity and extend the half-life, the VH domain was fused with human IgG1 Fc protein to form proteins of a bivalent format (VH-Fc). VH-Fc proteins were purified from transfected Expi293 cells and exhibit yields ranging 40-60 mg/L. VH-Fc 3C9 exhibits an EC50 of less than 1 nM (Figure 1C) in ELISA. VH-Fc 3C9 binds two different MSLN positive cell lines in a dose dependent manner (Figure 1D). In the SPR assay, the KD of VH-Fc 3C9 was 7 nM (Figure 1E). The reduced avidity is probably caused by the fixed orientations of VHs by the Fc protein [19].

A membrane proteome array (MPA) platform was used to test specificities of VH-Fc 3C9 against a total 6,000 different human membrane proteins including 94% of all single-pass, multi-pass, and GPI-anchored proteins (GPCRs, ion channels, and transporters) in a high-throughput screening manner based on flow cytometry. Cell specific binding was first verified in a dose dependent manner and was validated before the MPA assay. After verification and validation, the sample was run on the MPA assay. VH-Fc 3C9 showed no off target binding to 6,000 membrane associated proteins tested, demonstrating its low probability for non-specific toxicity as candidate for clinical therapeutic studies (Figure 1F).

Structural determination of MSLN-3C9 complex

3C9 stabilized the human recombinant MSLN, allowing us to co-crystallize the complex to understand antigen binding mechanisms. We were able to resolve the 3C9-MSLN complex at 2.9 Å (Table 1). The data clearly show two VH 3C9 domains, VH_1 and VH_2, indicating binding at 1:2 MSLN: VH 3C9 stoichiometry (Figure 2A). In addition,

in the crystal form, the C-terminal beta-strand in a VH domain inserts to the other VH domain (Figure 2B). This swapping of the C-terminal strand is similar to that previously observed [20]. Importantly, the identified interaction sites do not include the known glycosylation sites, residues 388, 488 and 515. Importantly, compared to the previously determined Amatuximab Fab complex with the N-terminal 67-amino acids of MSLN, VH domains extend the interaction site beyond the N-terminal 67-residues (Figure 2A). Indeed, VH 3C9 has no competition with Amatuximab in a competitive ELISA (Figure 2C). The details of full length MSLN and binding sites will be provided upon request after formal submission to a peer-reviewed journal.

VH domain based CAR-T cells, DDCs exhibit tumor cytotoxicity effects *in vitro*

MSLN specific m912 ScFv CAR-T has previously demonstrated therapeutic potential in both *in vitro* and *in vivo* studies [21]. To test the efficacy of CAR-T cells generated with VH domains, we constructed second generation CAR constructs based on the VH domain 3C9. Transduced T cells displayed ~ 60% CAR surface expression (Figure 3A). Despite donor heterogeneity, 3C9-CAR transduced T cells mediated superior antigen-specific killing of MSLN positive AsPC-1 and NCI-H2452 cells compared with untransduced T cells and did not kill MSLN negative 293T cells nonspecifically (Figure 3B). Domain drug conjugates have been discussed recently in different tumor models [18]. Exposed lysine based conjugation is a widely used non-specific conjugation strategy in DDC development with two lysine based ADCs having been approved by the FDA [22-24]. We recruited VH-Fc format antibody proteins for conjugation with a protease-labile valine-citrulline linker (OSu-Glu-vc-PAB-) linked with monomethyl auristatin E (MMAE) or a pH cleavable linker (CL2A) with SN-38 as payload to constitute VHFc-MMAE/SN38 conjugation. Both VH-Fc 3C9-MMAE and VH-Fc 3C9-SN-38 killed MSLN positive tumor cells toxicity without off-target effect in non-MSLN cells (Figure 3C). Based on the results collected, we conclude that the efficacy of DDCs will be affected by the conjugation approaches as well as the drug to antibody ratios. We are optimizing the DDC efficacies and *in vivo* distribution and efficacy assay are under assessment.

Discussion:

Several antibody therapeutics have shown limited anti-tumor activities in clinical trials. Amatuximab with strong ADCC effect showed moderate antitumor activity (NCT02357147). Immunotoxins such as SS1P (NCT01362790) can elicit neutralizing antibodies which largely affects the efficacy. Promising antitumor activity of MSLN-specific CAR T-cell therapy in combination with anti-PD1 therapy was observed in malignant pleural mesothelioma (MPM) (NCT02414269), lighting a hope for antibody therapeutics against MSLN. A panel of antibody drug conjugates was also reported

exhibiting manageable safety and encouraging preliminary antitumor activity in MSLN positive solid tumors (NCT01439152, NCT01469793 and NCT02341625).

Antibodies with satisfactory specificity and high affinity are critical to successful therapeutic development. Specificity of mAbs is one key issue that impacts the efficacy of antibody drugs because non-specific interactions can lead to off-target binding which results in toxicity or fast antibody clearance *in vivo* [25]. 3C9 did not bind the 6,000 human membrane-associated proteins in the MPA assay, demonstrating the comparably low potential for off-target toxicity. Although a potential limitation of human antibody VH domains is the lack of sufficient binding affinity required by therapeutic application, both VH and VH-Fc 3C9 showed less than 10 nM dissociation constant against MSLN. Based on the structure study about the binding site, 3C9 can be further increase its affinity by extending CDR3 region to fill the cavity (data not shown).

The antitumor activity for anti-MSLN ADCs with low off-target toxicity is encouraging in recent studies. DMOT4039A (h7D9.v3) is an MMAE conjugated humanized IgG1 anti-mesothelin mAb with promising antitumor activity and an acceptable safety profile based on a completed phase I study (NCT01469793). Anetumab ravtansine, another anti-MSLN ADC linked to maytansinoid DM4 exhibited a manageable safety profile in heavily pretreated patients with mesothelin-expressing solid tumors [26]. Compared with full length IgGs, VH and VH-Fc antibody formats have reduced the size that can be beneficial for penetration of solid tumors. In the present study, MMAE or SN38 conjugated VH-Fc proteins (either by lysine based conjugation or cysteine based conjugation, respectively) exhibit specific killing in MSLN positive tumor cells without off-target killing in MSLN negative cells. Human serum albumin (HSA) fused protein with a VH antibody is another option for the extension of half-life with a size and molecular weight (~80.5 kDa) similar to VH-Fc (~80 kDa) but remains monovalent whereby providing flexibility for therapeutic development upon design (e.g. bispecific antibody). HSA-VH based therapeutics avoid the quick elimination of VH protein by the circulatory system in vivo, and simultaneously eliminate Fc induced effector functions.

Several bi-paratopic antibodies have been reported in different tumor models [27-30]. In a breast cancer model, a bi-paratopic antibody shows enhanced avidity and cross linking activity to promote HER2 clustering and lysosomal degradation [27]. Since epitope of 3C9 is quite close to the epitopes of Amatuximab Fab, and there is no competition observed between 3C9 and Amatuximab, a biparatopic antibody designed including VH 3C9 and Fab Amatuximab may further increase the avidity without significant increase of antibody size [27, 28].

Clinical trials using MSLN-directed CAR T cells using a single-chain variable fragment (ScFv) format have demonstrated potential but with limited effect [10, 11, 21, 31]. No MSLN-directed CAR T cells based on the VH domain has been reported yet. We designed CAR constructs based on VH domain 3C9 recruiting 4-1BB as the signaling component. Although CD28 containing CAR-T cells show rapid elimination of tumors,

4-1BB containing CAR-T cells induce long-term remission with longer persistence [32]. In prostate cancer, 4–1BB-containing PSCA-directed CAR T cells show more durable antitumor responses compared with CD28-containing CAR T cells [11, 33]. In ovarian cancer, both CD28- and 4–1BB-containing CAR T cells were able to control SKOV3 cells and prolong the mice survival [21]. In our study, 4–1BB-containing VH 3C9 CAR T cells were effective in inducing tumor toxicity *in vitro* with 40%-80% killing of both AsPC-1 cells (pancreatic cancer) and NCI-H2452 (mesothelioma) without off target toxicity, demonstrating the possibility of using a VH domain in a CAR construct.

Immune escape by tumors can occur through multiple mechanisms such as antigen loss or binding escaping mutations within the same antigen [34, 35]. Multispecific CAR-T cells potentntly eliminate antigen-heterogeneous B cell tumors in preclinical models to conquer the relapse caused by antigen loss or down-regulation [36]. Bi-paratropic CARs or ADCs can target mutant variants simultaneously. Optimization of the CAR construct can further increase the efficacy. In one recent study, a CD19 specific CAR was designed inside T cell receptor–CD3 complex targeting cell surface antigens of low abundance (<20 antigens per cell) [35]. We are testing our 3C9 CAR-Ts based on the similar strategy. Combining CAR therapy with the use of checkpoint blockades to overcome CAR T-cell inhibition is another option to increase the efficacy. One phase II study combining MSLN CAR (m912 ScFv based) T-cell treatment in MPM with pembroluzimab is ongoing (NCT02414269).

In summary, we isolated and characterized a novel antibody VH domain with high affinity to MSLN, aggregation resistance, and satisfactory specificity. VH domain 3C9 can be used as CAR-T and ADC for tumor specific toxicity. Pharmacokinetic studies and animal trials of mono-topic/bi-paratopic CAR-T and ADCs are in progress to further evaluate clinical developability. It is also the first time to report the analysis of full length MSLN based on the crystal of MSLN-antibody complex. The PDB file will be subject to submission after a peer reviewed journal accepts our manuscript.

Methods:

Expression and purification of MSLN protein, VH binders, and VH bivalent proteins

The gene of human mesothelin was synthesized by IDT (Coralville, Iowa) with the sequence obtained from Uniprot (https://www.uniprot.org/uniprot/Q13421). The MSLN domain (residues 296-606) were cloned into an expression plasmid. This plasmid contains a CMV promotor and woodchuck posttranscriptional regulatory elements with a His tag. Proteins were purified by Ni-NTA (GE Healthcare). MSLN specific VH domains were in the pComb3x vector and purified from Escherichia coli HB2151 bacterial culture at 30°C for 16 h with stimulation by 1 mM IPTG. Cells were lysed by Polymyxin B (Sigma-Aldrich). Lysates were spun down and supernatant was loaded over Ni-NTA (GE Healthcare). For conversion to Fc-fusion, the VH gene was re-amplified and re-cloned into pSectaq vector containing human Fc. VH-Fc

proteins were expressed in the Expi293 expression system (Thermo Fisher Scientific) and purified with protein A resin (GenScript). Buffer replacement in protein purification used Column PD 10 desalting column (GE Healthcare). All protein purity was estimated as >95% by SDS-PAGE and protein concentration was measured spectrophotometrically (NanoVue, GE Healthcare). Further details can be found in our previous publication [19].

ELISA and SPR

For ELISA assays, antigen protein was coated on a 96-well plate (Costar) at 50 ng/well in PBS overnight at 4°C. For the soluble VH binding assay, horseradish peroxidase (HRP)-conjugated mouse anti-FLAG tag antibody (A8592, Sigma-Aldrich) was used to detect VH binding. For detection of human Fc protein, HRP-goat anti-human IgG Fc secondary antibody (A18817, Thermo Fisher Scientific) was used. For the competition ELISA, 200 nM of IgG1 m912, or 50 nM VH-Fc 3C9 was incubated with serially diluted VH proteins, and the mixtures were added to antigen-coated wells. After washing, competition was detected by HRP-goat anti-human IgG Fc secondary antibody (A18817, Thermo Fisher Scientific). The kinetics of the antibody fragments were determined using a Biacore X100 (GE Healthcare). Human MSLN (Advance BioMatrix 5123-0.1mg) was (10 mg/mL) was immobilized onto a CM5 sensor chip (GE Healthcare, BR100012) by amine coupling. The antibody fragments diluted in HBS-EP buffer (10 mM HEPES, 150 mM NaCl, 3 mM EDTA, and 0.005% surfactant P20, pH 7.4) were injected over an immobilized surface (200 - 400 RU) for 90 sec at a rate of 50 µL/min, followed by dissociation for 600 sec. After each sample injection, the surface was regenerated by injection of regeneration solution (10 mM Glycine/ 10% Glycerol pH 2.0 for VH and VH-Fc binders; 0.5 M guanidine hydrochloride at pH 3.0 for bi-paratopic VH-Fc binders). The kinetic values, ka, kd, and KD were calculated using the BiacoreX100 Evaluation Software (GE Healthcare).

ADC generation

Monomethyl auristatin E (MMAE) was conjugated to VH-Fc 3C9 via the cross-linker OSu-Glu-VC-PAB (SET0100, Levena Biopharma, USA) with a molar ratio mAb:OSu-Glu-VC-PAB-MMAE of 1:10. The conjugation was performed in buffer composed of 50 mM potassium phosphate, 50 mM sodium chloride, and 2 mM EDTA (pH 6.5) with the reaction run for 18-24 h at room temperature. The reaction was stopped by adding 50 mM sodium succinate (pH 5.0) followed by buffer replacement by using Column PD 10 desalting column (GE Healthcare). Antibody SN-38 drug conjugates were prepared using purified antibody [37]. Briefly, antibodies were reduced using a 100X molar excess of TCEP (Millipore-Sigma CAT#580561) followed by reformation using 20 equivalents of dehydroascorbic acid (Millipore Sigma CAT# 261556). Rather than adjusting pH using titration, buffers were changed using a PD-Minitrap G25 column (Cytiva CAT#28918007). Antibody was similarly diluted 1:1 (v/v) with propylene glycol (Millipore Sigma CAT# P4347) and 3 equivalents of CL2A-SN-38 (Cayman Chemical CAT#33941) were added and incubated overnight at 4°C. The protein was washed and concentrated using 30 kDa Amicon centrifugal filter unit (Millipore Sigma CAT#UFC8030).

CAR-T cell preparation

MSLN-directed CAR constructs containing different human MSLN-specific VH followed by 4–1BB-CD3ζ signaling domain. T cells from healthy donors were transduced with γ-retroviral vectors encoding CAR constructs. CAR transduction efficiency was determined by flow cytometry with CAR expression detected by human MSLN staining. Retroviral supernatant production and activation and viral transduction of T cells was performed as described previously [38].

Cell Viability Assays

Cell viability was measured using CellTiter-Glo (G7570, Promega). Briefly, MSLN positive or negative cells were plated into 96-wells, allowing attachment and growth for 24 hr, then triplicate wells were treated with ADCs, naked antibodies, free drugs, or ADCs plus competitor antibodies. Three to five days later, when untreated control wells were 70 to 90% confluent, reagent was added to the plates according to the supplier's instructions. Wells treated identically but wells without cells were used to subtract background. Fluorescence (ex: 570 nm, Em: 585 nm) was measured using a CLARIOstar microplate reader (BMG Labtech) and data analyzed using GraphPad Prism 8 software. Significance was tested using one-way ANOVA, followed by the Tukey's multiple post hoc test. ****$P < 0.0001$; ***$P < 0.001$; **$P < 0.01$; *$P < 0.05$ versus antibody isotype control (VH-Fc 3C9) at each concentration. For the CAR-T cells killing assay, untransduced T cells were used as control. Percentage of lysis of MSLN+ tumor cell lines (NCI-H2452 and Aspc-1) by 3C9 CAR T cells measured by LDH release assays (n = 4–9) (J2380, Promega) **, $P < 0.01$; ***, $P<0.001$; ****, $P<0.0001$ versus untransduced T cells at each dose.

Size Exclusion Chromatography (SEC)

The Superdex 200 Increase 10/300 GL chromatography (GE Healthcare, Cat. No. 28990944) was used for loading samples. The column was calibrated with protein molecular mass standards of Ferritin (Mr 440 000 kDa), Aldolase (Mr 158 000 kDa), Conalbumin (Mr 75 000 kDa), Ovalbumin (Mr 44 000 kDa), Carbonic anhydrase (Mr 29 000 kDa), Ribonuclease A (Mr 13 700 kDa). 150 µl filtered proteins (1-2 mg/ml) in PBS were used for analysis. Flow rate was 0.4 ml/min.

Membrane Proteome Array

Integral Molecular, Inc. (Philadelphia, PA) performed specificity testing of VH-Fc 3C9 using the Membrane Proteome Array (MPA) platform. The MPA comprises 5,300 different human membrane protein clones, each overexpressed in live cells from expression plasmids that are individually transfected in separate wells of a 384-well plate (Tucker et al., 2018). The entire library of plasmids is arrayed in duplicate in a matrix format and transfected into HEK293T cells, followed by incubation for 36 h to allow protein expression. Before specificity testing, optimal antibody concentrations for screening were determined by using cells expressing positive (membrane-tethered Protein A) and negative (mock-transfected) binding controls, followed by flow cytometric detection with an Alexa Fluor-conjugated secondary antibody (Jackson ImmunoResearch Laboratories). Cell specific binding was confirmed first. Based on the assay setup results, VH-Fc protein (20 µg/ml) was added to the MPA. Binding across the protein library was measured on an iQue3 (Ann Arbor, MI) using the same fluorescently

labeled secondary antibody. To ensure data validity, each array plate contained positive (Fc-binding; MSLN protein) and negative (empty vector) controls. Identified targets were confirmed in a second flow cytometric experiment by using serial dilutions of the test antibody. The identity of each target was also confirmed by sequencing.

Crystallization

MSLN complex with VH 3C9 was prepared by injecting the protein mixture to Superdex 75 column (GE Healthcare, Chicago IL), and concentrated to 12 mg/mL. To allow multi-wavelength anomalous diffraction analysis, selenomethionine (Se-Met) labeled VH 3C9 was also prepared by expressing the protein in E.Coli BL21(DE3) cells, using a minimum media with Se-Met and supplemental amino acids to reduce Se-Met toxicity (L-isoleucine, L-leucine, L-lysine, L-phenylalanine, L-threonine, and L-valine) prior to the induction [39]. The Se-Met incorporation to VH 3C9 was confirmed by mass spectrometry, 15122.52 Da (theoretical mass, 15123.23 Da), by comparing the mass without Se-Met labeling, 15028.68 Da (theoretical mass 15029.41 Da), using a LC–TOF mass spectrometry (Bruker Daltonics, Billerica, MA). Data were collected at the 12-2 SSRL (wavelength 0.9795 Å). Diffraction data were processed, integrated and scaled using XDS. The structure was solved by single-wavelength diffraction analysis. Model building and refinement were performed using Coot and Phenix [40, 41] (Table 1).The complex structure will be deposited to the Protein Data Bank.

Author Contributions

Z.S. and D.S.D. designed project. Zehua identified and characterized antibodies, designed CAR-T, DDCs and *in vivo* assay. X.C. produced recombinant MSLN proteins for crystallization study. C.A. performed UPLC for DAR determination and cell cytotoxicity assays. C.C. produced the VH-Fc protein for assay. D.J. and W.L. studied the modeling of epitope of antibody. T.I.. R.I., and G.C did crystallization. R.I. conducted SPR experiments. S.V. and G.C. determined crystal structure. Z.S. wrote the first draft of the article. C.A. revised the draft. Z.S., J.W.M., and D.S.D. discussed the results and further revised the manuscript. All authors contributed to the final manuscript.

Acknowledgments

We would like to thank the members of the Center for Antibody Therapeutics in University of Pittsburgh for their helpful discussions. We thank Michel Guerrero to support the crystallization, and Andrew Hinck for the use of the Biacore X100 instrument. This work was supported by the University of Pittsburgh Medical Center.

Declaration of Interests

Z.S., J.W.M., and D.S.D. are co-inventors of a patent, filed on March 12 by the University of Pittsburgh, related to 3C9 described in this paper.

Figure legends:

Figure 1. Characterization of 3C9. A. SEC data of both VH and VH-Fc 3C9. VH and VH-Fc ab8 was used as control for aggregation. B-C. ELISA of VH/VH-Fc binders binding to human MSLN. D. Cell specific binding assay by VH-Fc 3C9 in a dose dependednt manner. E. SPR of 3C9 VH and the VH-Fc forms. F. Lack of non-specific binding measured by a Membrane Proteome Array (MPA). Antibody domain 3C9 was fused human Fc protein for the examination by flow cytometry. VH-Fc 3C9 (20 µg/ml) was tested in a Membrane Proteome Array against 6,000 different human membrane proteins.

Figure 2. Structure of MSLN-3C9 complex, determined by crystallography. A. MSLN, (coordinate shown from residue 300 to 582, purple), complex with two VH 3C9 domains, VH_1 and VH_2 (blue and green, respectively). B. The same structure, highlighting swapping of the C-terminal beta-strands in two VH 3C9 domains. C. VH 3C9 and Amatuximab have no competition in competing ELISA.

Figure 3. Characterization of MSLN-directed CAR T cells and DDCs *in vitro* toward MSLN positive human pancreatic cancer cell line and lung mesothelioma. A. VH domain/ScFv CARs expression measured by flow cytometry in CAR T cells three days after transduction. B. Percentage of lysis of MSLN+ tumor cell lines (NCI-H2452 and Aspc-1) by 3C9 CAR T cells measured by LDH release assays (n = 4–9). **, P < 0.01; ***, P<0.001; ****, P<0.0001. C. Efficacy of DDCs in killing tumor cells and non MSLN cells *in vitro*. ****P < 0.0001; ***P < 0.001; **P < 0.01; *P < 0.05 versus antibody isotype control (VH-Fc 3C9) at each concentration.

Table 1. Data collection, phasing and refinement statistics

	SSRL (12-1)
Data collection	
Space group	$P4_322$
Cell dimensions	
a, *b*, *c* (Å)	114.1 114.1 340.7
α, β, γ (°)	90, 90, 90
Resolution (Å)	60-2.9
R_{sym} or R_{merge}	0.008(0.45)

I / σI – CC1/2	27.5(1.1) – 99(35)
Completeness (%)	100(100)
Redundancy	25(18)
Phasing	
Wavelength (Se peak)	0.9794
No of sites	8
FOM (SAD)	0.27
Refinement	
Resolution (Å)	37-2.9
No. reflections	51008
R_{work} / R_{free}	22.1/24.4
B-factors	
Protein	65.5
Ligand/ion	N/A
Water	74
R.m.s. deviations	
Bond lengths (Å)	0.009
Bond angles (°)	1.33

*Values in parentheses are for highest-resolution shell.

Reference

1. Hassan, R., et al., *Detection and quantitation of serum mesothelin, a tumor marker for patients with mesothelioma and ovarian cancer.* Clin Cancer Res, 2006. **12**(2): p. 447-53.
2. Chang, K., I. Pastan, and M.C. Willingham, *Isolation and characterization of a monoclonal antibody, K1, reactive with ovarian cancers and normal mesothelium.* Int J Cancer, 1992. **50**(3): p. 373-81.
3. Pastan, I. and R. Hassan, *Discovery of mesothelin and exploiting it as a target for immunotherapy.* Cancer Res, 2014. **74**(11): p. 2907-12.
4. Hassan, R., et al., *Phase 1 study of the antimesothelin immunotoxin SS1P in combination with pemetrexed and cisplatin for front-line therapy of pleural mesothelioma and correlation of tumor response with serum mesothelin, megakaryocyte potentiating factor, and cancer antigen 125.* Cancer, 2014. **120**(21): p. 3311-9.
5. Ordonez, N.G., *Application of mesothelin immunostaining in tumor diagnosis.* Am J Surg Pathol, 2003. **27**(11): p. 1418-28.
6. Hassan, R., et al., *Mesothelin is overexpressed in pancreaticobiliary adenocarcinomas but not in normal pancreas and chronic pancreatitis.* Am J Clin Pathol, 2005. **124**(6): p. 838-45.
7. Hassan, R., et al., *Localization of mesothelin in epithelial ovarian cancer.* Appl Immunohistochem Mol Morphol, 2005. **13**(3): p. 243-7.
8. Nichetti, F., et al., *The Role of Mesothelin as a Diagnostic and Therapeutic Target in Pancreatic Ductal Adenocarcinoma: A Comprehensive Review.* Target Oncol, 2018. **13**(3): p. 333-351.
9. Hassan, R., T. Bera, and I. Pastan, *Mesothelin: a new target for immunotherapy.* Clin Cancer Res, 2004. **10**(12 Pt 1): p. 3937-42.
10. Zhao, X.Y., et al., *Novel Antibody Therapeutics Targeting Mesothelin In Solid Tumors.* Clin Cancer Drugs, 2016. **3**(2): p. 76-86.
11. Adusumilli, P.S., et al., *Regional delivery of mesothelin-targeted CAR T cell therapy generates potent and long-lasting CD4-dependent tumor immunity.* Sci Transl Med, 2014. **6**(261): p. 261ra151.
12. Feng, Y., et al., *A novel human monoclonal antibody that binds with high affinity to mesothelin-expressing cells and kills them by antibody-dependent cell-mediated cytotoxicity.* Mol Cancer Ther, 2009. **8**(5): p. 1113-8.
13. Detalle, L., et al., *Generation and Characterization of ALX-0171, a Potent Novel Therapeutic Nanobody for the Treatment of Respiratory Syncytial Virus Infection.* Antimicrob Agents Chemother, 2016. **60**(1): p. 6-13.
14. Nessler, I., et al., *Increased Tumor Penetration of Single-Domain Antibody-Drug Conjugates Improves In Vivo Efficacy in Prostate Cancer Models.* Cancer Res, 2020. **80**(6): p. 1268-1278.
15. Jain, R.K., *Physiological barriers to delivery of monoclonal antibodies and other macromolecules in tumors.* Cancer Res, 1990. **50**(3 Suppl): p. 814s-819s.
16. Leyton-Castro, N.F., M.M. Brigido, and A.Q. Maranhao, *Selection of Antibody Fragments for CAR-T Cell Therapy from Phage Display Libraries.* Methods Mol Biol, 2020. **2086**: p. 13-26.
17. Winthrop, M.D., G.L. Denardo, and S.J. Denardo, *Antibody phage display applications for nuclear medicine imaging and therapy.* Q J Nucl Med, 2000. **44**(3): p. 284-95.
18. Sun, Z., et al., *Construction of a Large Size Human Immunoglobulin Heavy Chain Variable (VH) Domain Library, Isolation and Characterization of Novel Human Antibody VH Domains Targeting PD-L1 and CD22.* Frontiers in Immunology, 2022. **13**.
19. Sun, Z., et al., *Potent neutralization of SARS-CoV-2 by human antibody heavy-chain variable domains isolated from a large library with a new stable scaffold.* MAbs, 2020. **12**(1): p. 1778435.
20. Spinelli, S., et al., *Domain swapping of a llama VHH domain builds a crystal-wide beta-sheet structure.* FEBS Lett, 2004. **564**(1-2): p. 35-40.
21. Schoutrop, E., et al., *Mesothelin-Specific CAR T Cells Target Ovarian Cancer.* Cancer Res, 2021. **81**(11): p. 3022-3035.
22. Jen, E.Y., et al., *FDA Approval: Gemtuzumab Ozogamicin for the Treatment of Adults with Newly Diagnosed CD33-Positive Acute Myeloid Leukemia.* Clin Cancer Res, 2018. **24**(14): p. 3242-3246.
23. Wedam, S., et al., *FDA Approval Summary: Ado-Trastuzumab Emtansine for the Adjuvant Treatment of HER2-positive Early Breast Cancer.* Clin Cancer Res, 2020. **26**(16): p. 4180-4185.

24. Vaklavas, C. and A. Forero-Torres, *Safety and efficacy of brentuximab vedotin in patients with Hodgkin lymphoma or systemic anaplastic large cell lymphoma.* Ther Adv Hematol, 2012. **3**(4): p. 209-25.
25. Starr, C.G. and P.M. Tessier, *Selecting and engineering monoclonal antibodies with drug-like specificity.* Curr Opin Biotechnol, 2019. **60**: p. 119-127.
26. Golfier, S., et al., *Anetumab ravtansine: a novel mesothelin-targeting antibody-drug conjugate cures tumors with heterogeneous target expression favored by bystander effect.* Mol Cancer Ther, 2014. **13**(6): p. 1537-48.
27. Li, J.Y., et al., *A Biparatopic HER2-Targeting Antibody-Drug Conjugate Induces Tumor Regression in Primary Models Refractory to or Ineligible for HER2-Targeted Therapy.* Cancer Cell, 2019. **35**(6): p. 948-949.
28. Fan, J., et al., *A multivalent biparatopic EGFR-targeting nanobody drug conjugate displays potent anticancer activity in solid tumor models.* Signal Transduct Target Ther, 2021. **6**(1): p. 320.
29. DaSilva, J.O., et al., *A Biparatopic Antibody-Drug Conjugate to Treat MET-Expressing Cancers, Including Those that Are Unresponsive to MET Pathway Blockade.* Mol Cancer Ther, 2021. **20**(10): p. 1966-1976.
30. Pegram, M.D., et al., *First-in-Human, Phase 1 Dose-Escalation Study of Biparatopic Anti-HER2 Antibody-Drug Conjugate MEDI4276 in Patients with HER2-positive Advanced Breast or Gastric Cancer.* Mol Cancer Ther, 2021. **20**(8): p. 1442-1453.
31. Beatty, G.L., et al., *Activity of Mesothelin-Specific Chimeric Antigen Receptor T Cells Against Pancreatic Carcinoma Metastases in a Phase 1 Trial.* Gastroenterology, 2018. **155**(1): p. 29-32.
32. Zhao, Z., et al., *Structural Design of Engineered Costimulation Determines Tumor Rejection Kinetics and Persistence of CAR T Cells.* Cancer Cell, 2015. **28**(4): p. 415-428.
33. Priceman, S.J., et al., *Co-stimulatory signaling determines tumor antigen sensitivity and persistence of CAR T cells targeting PSCA+ metastatic prostate cancer.* Oncoimmunology, 2018. **7**(2): p. e1380764.
34. Anthony-Gonda, K., et al., *Multispecific anti-HIV duoCAR-T cells display broad in vitro antiviral activity and potent in vivo elimination of HIV-infected cells in a humanized mouse model.* Sci Transl Med, 2019. **11**(504).
35. Mansilla-Soto, J., et al., *HLA-independent T cell receptors for targeting tumors with low antigen density.* Nat Med, 2022. **28**(2): p. 345-352.
36. Schneider, D., et al., *Trispecific CD19-CD20-CD22-targeting duoCAR-T cells eliminate antigen-heterogeneous B cell tumors in preclinical models.* Sci Transl Med, 2021. **13**(586).
37. Jeffrey, S.C., et al., *A potent anti-CD70 antibody-drug conjugate combining a dimeric pyrrolobenzodiazepine drug with site-specific conjugation technology.* Bioconjug Chem, 2013. **24**(7): p. 1256-63.
38. Haso, W., et al., *Anti-CD22-chimeric antigen receptors targeting B-cell precursor acute lymphoblastic leukemia.* Blood, 2013. **121**(7): p. 1165-74.
39. Suzuki, M., et al., *Bacterial bioreactors for high yield production of recombinant protein.* J Biol Chem, 2006. **281**(49): p. 37559-65.
40. Emsley, P. and K. Cowtan, *Coot: model-building tools for molecular graphics.* Acta Crystallogr D Biol Crystallogr, 2004. **60**(Pt 12 Pt 1): p. 2126-32.
41. Liebschner, D., et al., *Macromolecular structure determination using X-rays, neutrons and electrons: recent developments in Phenix.* Acta Crystallogr D Struct Biol, 2019. **75**(Pt 10): p. 861-877.

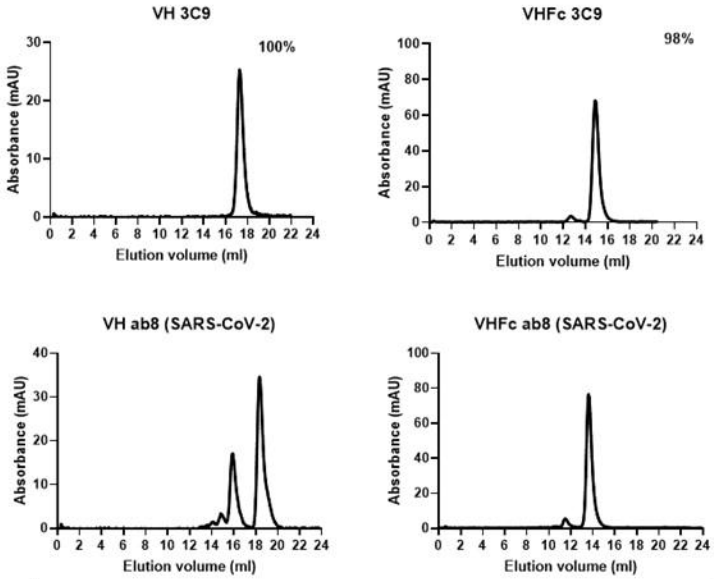
VH 3C9
100%
VHFc 3C9
98%
VH ab8 (SARS-CoV-2)
VHFc ab8 (SARS-CoV-2)
Absorbance (mAU)
Elution volume (ml)

A

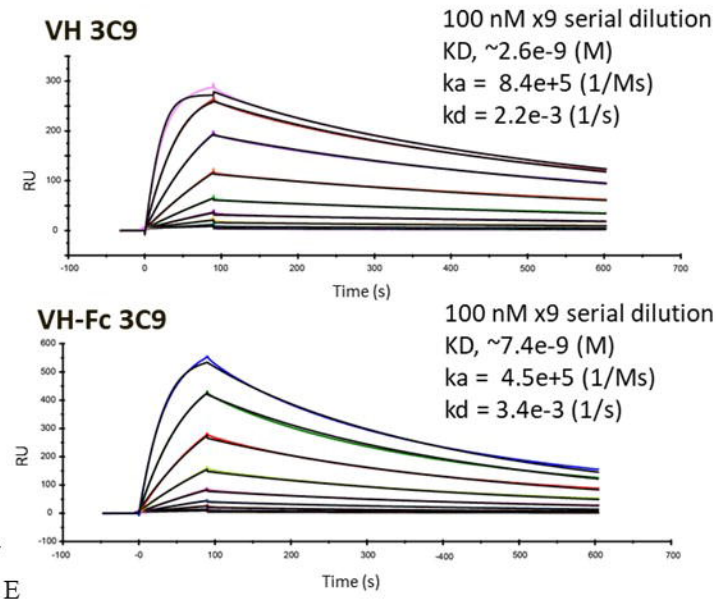
VH 3C9
100 nM x9 serial dilution
KD, ~2.6e-9 (M)
ka = 8.4e+5 (1/Ms)
kd = 2.2e-3 (1/s)
VH-Fc 3C9
100 nM x9 serial dilution
KD, ~7.4e-9 (M)
ka = 4.5e+5 (1/Ms)
kd = 3.4e-3 (1/s)
RU
Time (s)

E

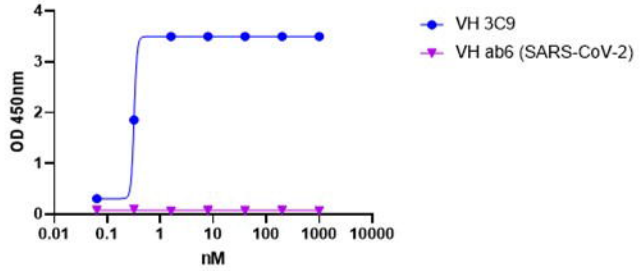
VH 3C9
VH ab6 (SARS-CoV-2)
OD 450nm
nM

B

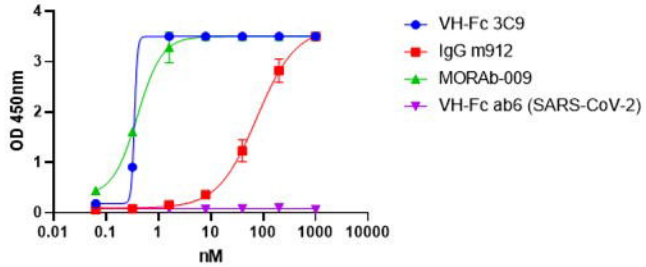
VH-Fc 3C9
IgG m912
MORAb-009
VH-Fc ab6 (SARS-CoV-2)
OD 450nm
nM

C

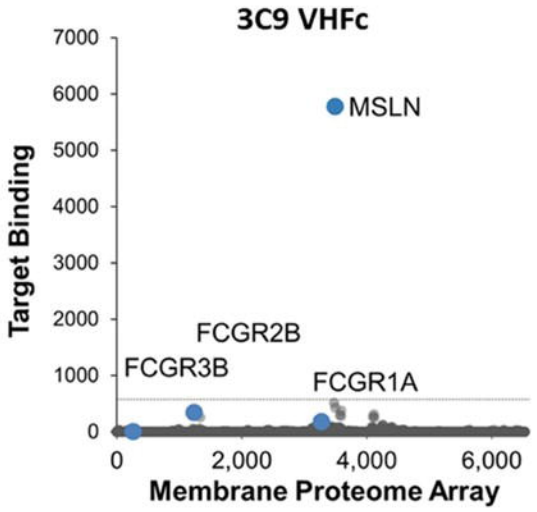
3C9 VHFc
MSLN
FCGR2B
FCGR3B
FCGR1A
Target Binding
Membrane Proteome Array

F

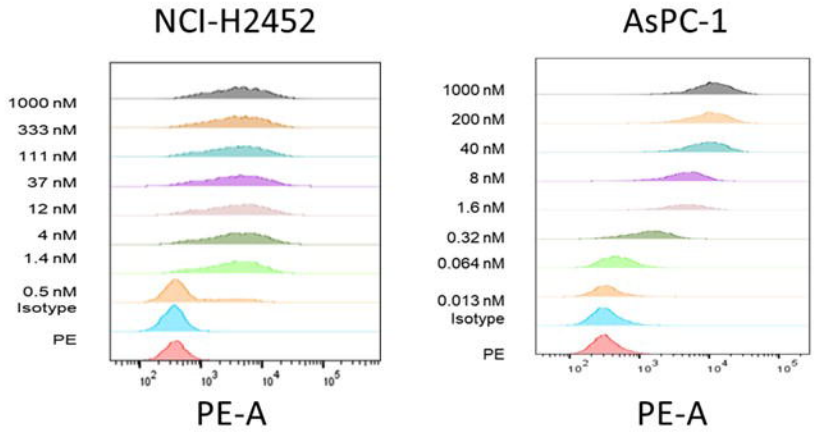
NCI-H2452
AsPC-1
1000 nM
333 nM
111 nM
37 nM
12 nM
4 nM
1.4 nM
0.5 nM
Isotype
PE
200 nM
40 nM
8 nM
1.6 nM
0.32 nM
0.064 nM
0.013 nM
PE-A

D

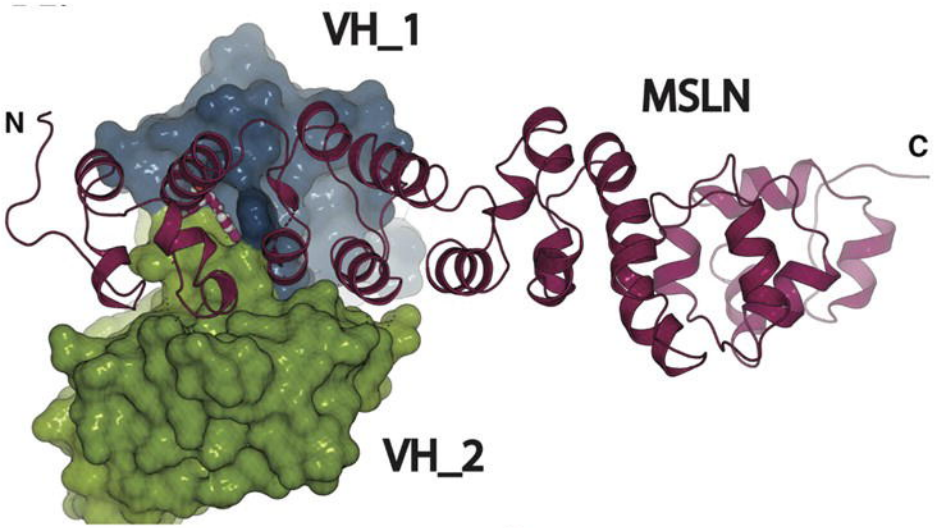
VH_1
MSLN
N
C
VH_2

A

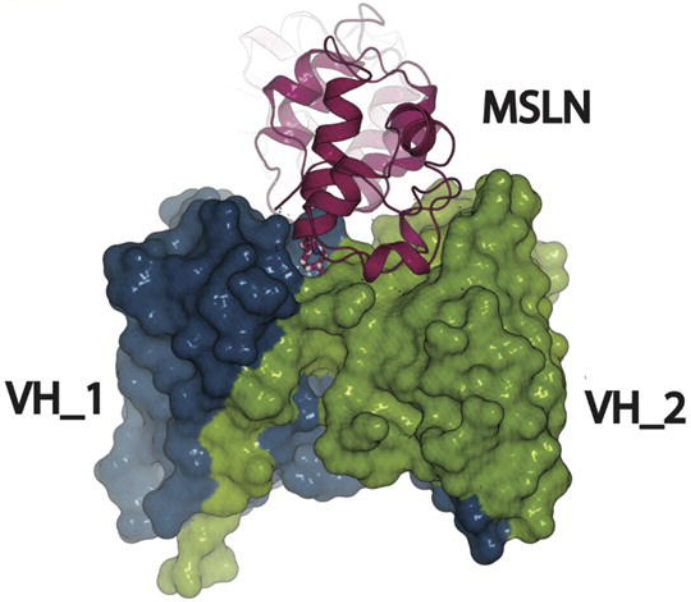
MSLN
VH_1
VH_2

B

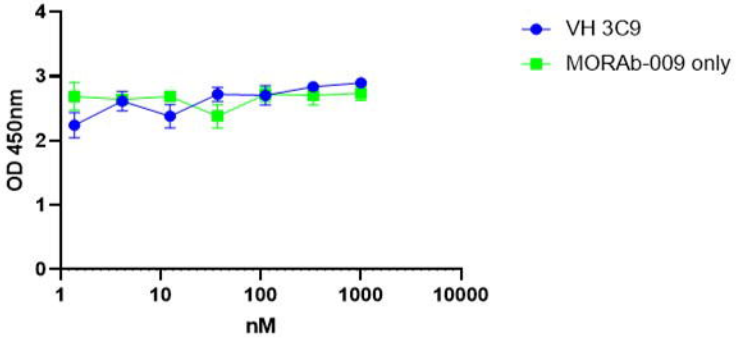
OD 450nm
0
1
2
3
4
1
10
100
1000
10000
nM
VH 3C9
MORAb-009 only

C

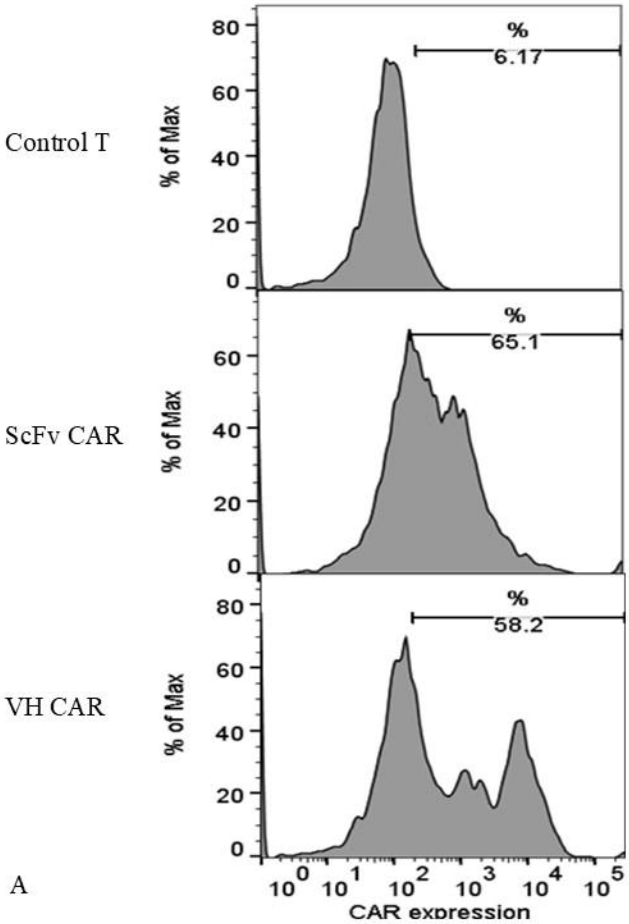
Control T
ScFv CAR
VH CAR
% of Max
%
6.17
65.1
58.2
CAR expression

A

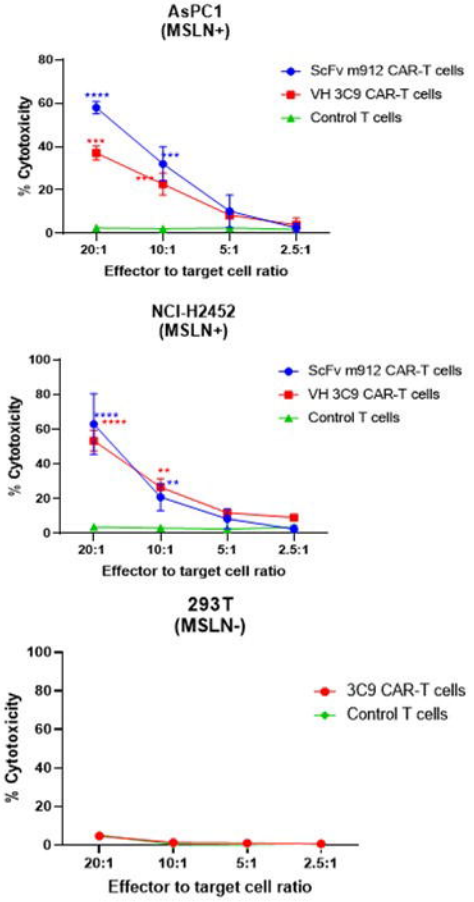
AsPC1
(MSLN+)
ScFv m912 CAR-T cells
VH 3C9 CAR-T cells
Control T cells
% Cytotoxicity
Effector to target cell ratio
NCI-H2452
(MSLN+)
293T
(MSLN-)
3C9 CAR-T cells
20:1
10:1
5:1
2.5:1

B

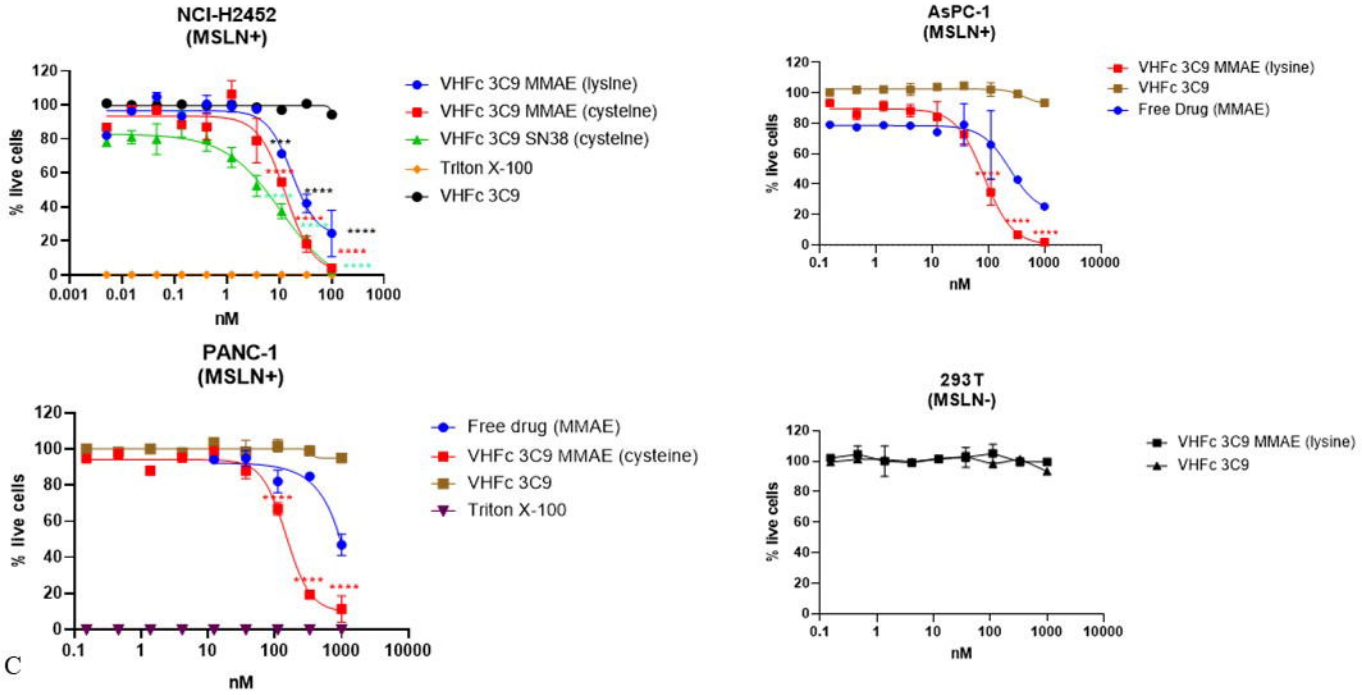
NCI-H2452
(MSLN+)
VHFc 3C9 MMAE (lysine)
VHFc 3C9 MMAE (cysteine)
VHFc 3C9 SN38 (cysteine)
Triton X-100
VHFc 3C9
AsPC-1
(MSLN+)
Free Drug (MMAE)
PANC-1
(MSLN+)
Free drug (MMAE)
293T
(MSLN-)
% live cells
nM

C